

Iron(II) Self-Assembled Molecular Systems as Electrochromic Devices

Jade Poisson, Heather Geoffrey, Alex Deckert, Jesse Allan, Iraklii Ebralidze, Olena Zenkina*, Brad Easton

Introduction

Introduced here are layer by layer self assembled coordination based molecular systems with organometallic layers. These systems have applications as electrochromic devices. Electrochromic devices are those that undergo a change in optical properties upon the application of an external stimulus such as potential or current¹. The organometallic complexes are composed of iron (II) metal centers with terpyridine derivative ligands. Terpyridine was chosen for its high affinity towards iron. Two terpyridine derivative ligands were chosen for this purpose, the first is 4',4''''-(1,4-Phenylene)bis(2,2':6,2''-terpyridine) which is expected for form a wire perpendicular to the ITO glass support. The second ligand used was 4',4''''-(((6-chloro-1,3,5-triazine-2,4-diyl)bis(oxy))bis(4,1-phenylene))di-2,2':6',2''-terpyridine which is expected to form a zig-zag type wire.

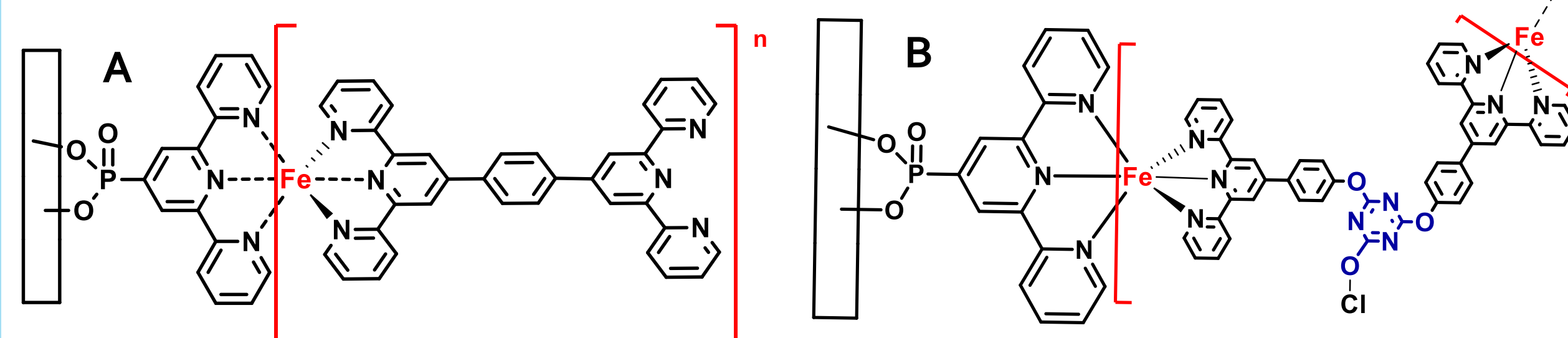


Figure 1: the structures of the Iron(II) assemblies. A) the bisterpyridine assembly. B) the triazine terpyridine assembly.

Experimental Methods

Layer formation-

The molecular wires were built on Indium tin oxide conducting glass slides cleaned with basic piranha solution. The anchoring ligand, [2,2':6',2''-terpyridin]-4-ylphosphonic acid was deposited onto the slides for 8 hours (a 0.64 mM solution in chloroform). A 1.0 mM solution iron(II) perchlorate in ethanol was deposited onto the slides for 24 hours. Followed by an 8 hour deposition of a the ligand solution (0.19 mM for bisterpy and 0.30 mM for the triazine in chloroform). One iron and ligand deposition represents one layer. All depositions were conducted under ambient conditions.

Electrochemistry-

DPV, CV and EIS analysis was performed in solution the electrolyte used was a 0.1 M TBAHFP solution in ACN. The SEC analysis was performed in the solid state, the electrolyte was a gel (of potassium trifluoromethanesulfonate in ACN with PVB as the binder). A pine research wavedriver 10 potentiostat was used for differential pulse voltammetry and spectroelectrochromic analysis, a Solartron Analytical 1287 Potentiostat/Galvanostat was used for cyclic voltammetry and spectroelectrochromic analysis.

UV-Visible spectrophotometry-

The samples were measured using a Perkin Elmer Lambda 760 diffuse reflectance spectrophotometer for both UV-Visible analysis and spectroelectrochromic analysis.

Results

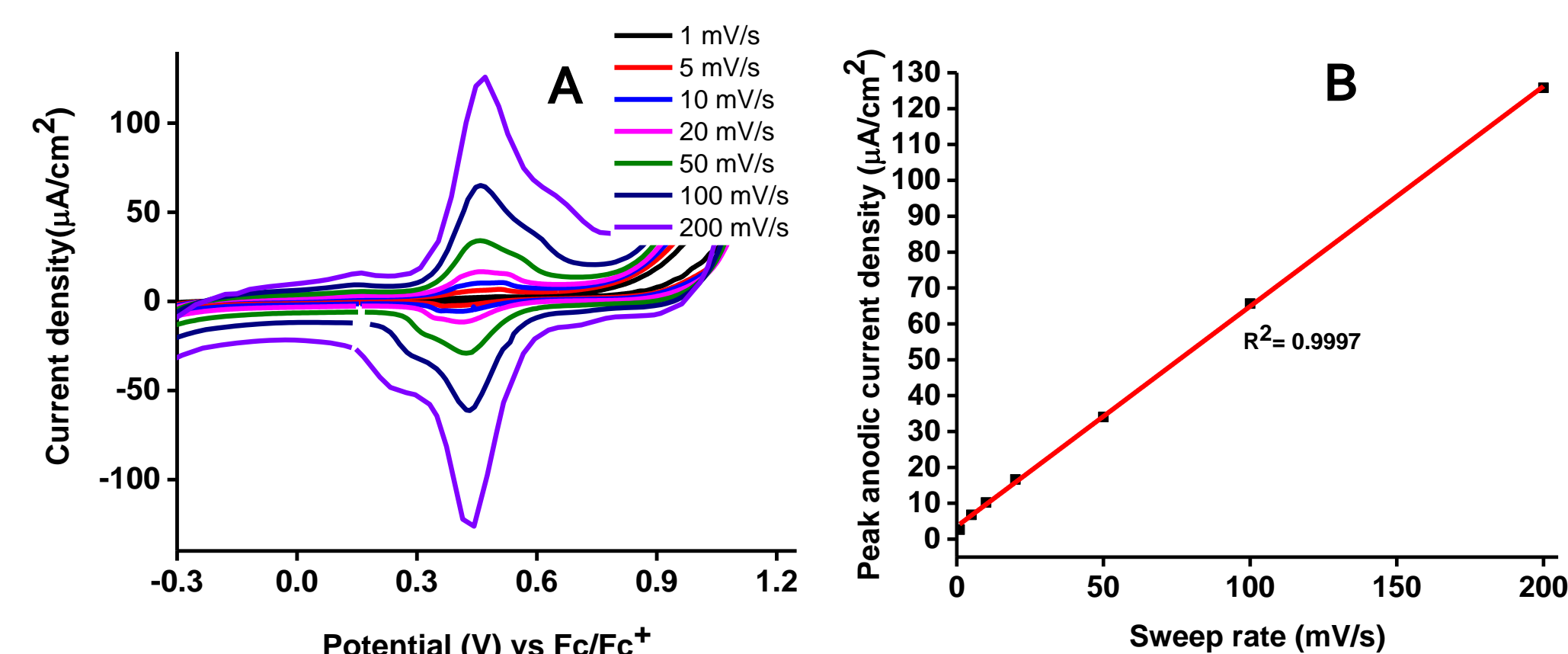


Figure 2: the cyclic voltammetry results for layer 12 of the bisterpyridine assembly. A) the voltammograms for the variable sweep rates. B) the plot of sweep rate vs peak anodic current.

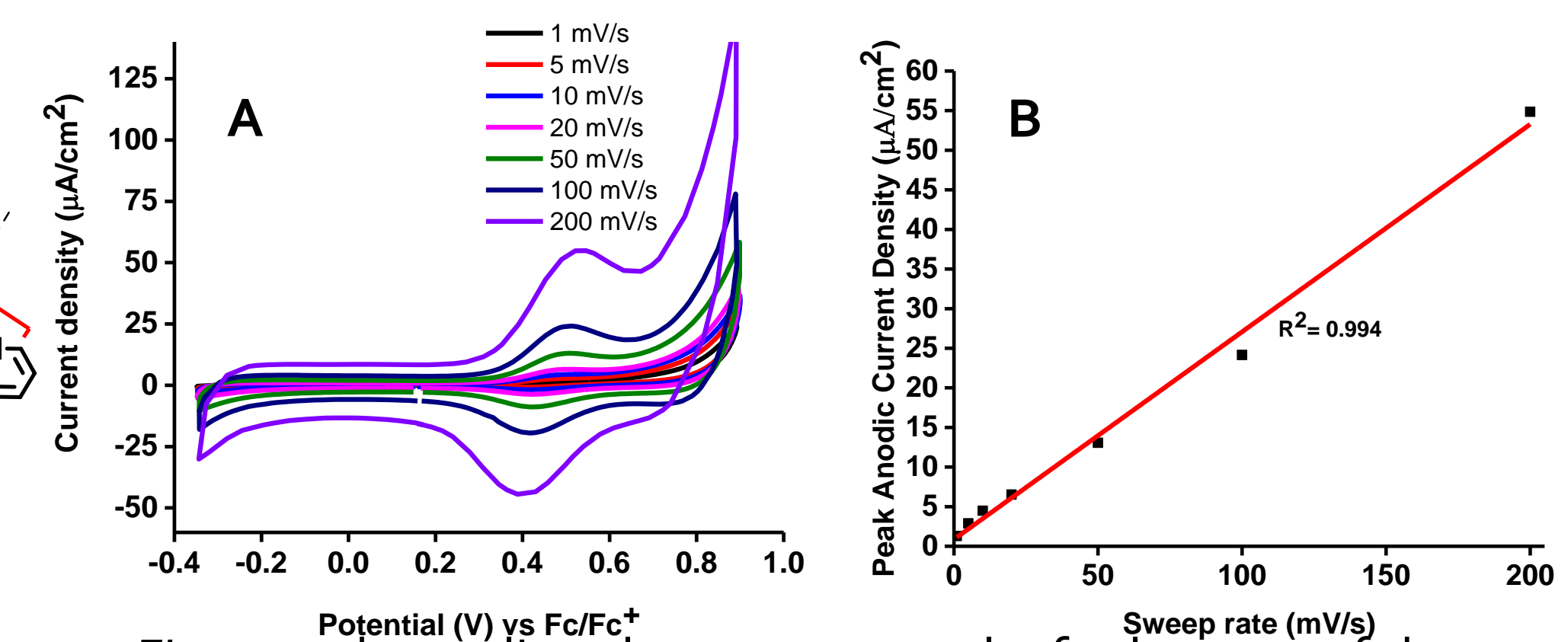


Figure 3: the cyclic voltammetry results for layer 12 of the triazine terpyridine assembly. A) the voltammograms for the variable sweep rates. B) the plot of sweep rate vs peak anodic current.

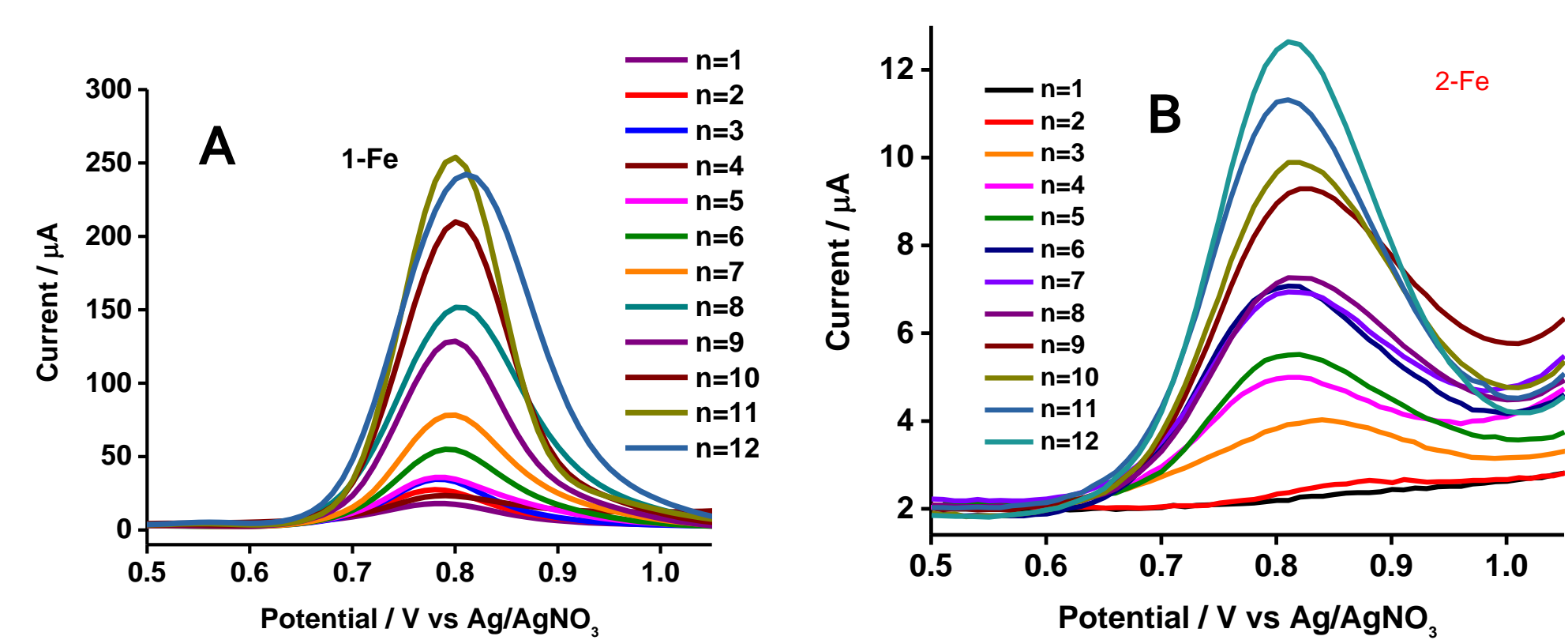


Figure 4: the differential pulse voltammetry results for all of the layers of each assembly. A) the bisterpyridine assembly B) the triazine terpyridine assembly

Conclusions

The UV-visible and differential pulse voltammetry results indicate that the amount of iron increases with increasing layers which proves that the layers are being propagated. Furthermore, since the cyclic voltammetry plot of layers versus peak anodic current are linearly related in both assemblies, this indicates that up to layer 12, the kinetics of the system is dictated by thin layer behavior which shows that the electrons travel is not limited by diffusion. Additionally, the UV-Visible and DPV results prove that the bisterpyridine assembly grows more rapidly with increasing layers likely due to the wire orientation.

From the spectroelectrochromic data it is evident that the systems are stable over the first several hours of continuous reductive-oxidative switching. This is indicated by the fact that the change in absorbance between the reductive and oxidative states is constant for the first several hours after which both films appear to undergo degradation of the wire. However, although the bisterpy can undergo extremely fast reductive-oxidative switching (with some loss of optical density) the triazine terpy system cannot without compromising the resolution and degrading the film. This analysis shows that the bisterpy assembly has a greater capacity for electrochromic properties.

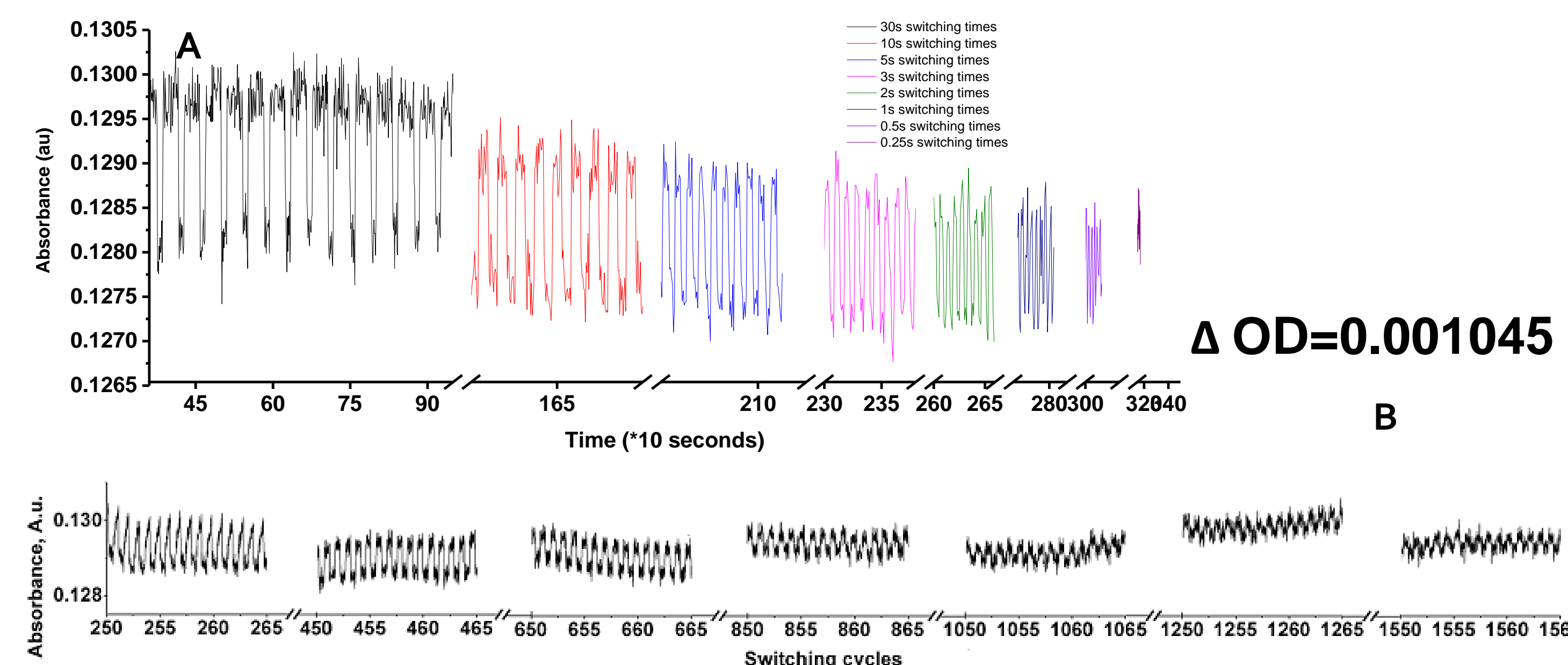


Figure 5: the spectroelectrochromic data for the triazine terpyridine assembly. A) the switching time cycles. B) a subsection of the long term cycling for 48 hours.

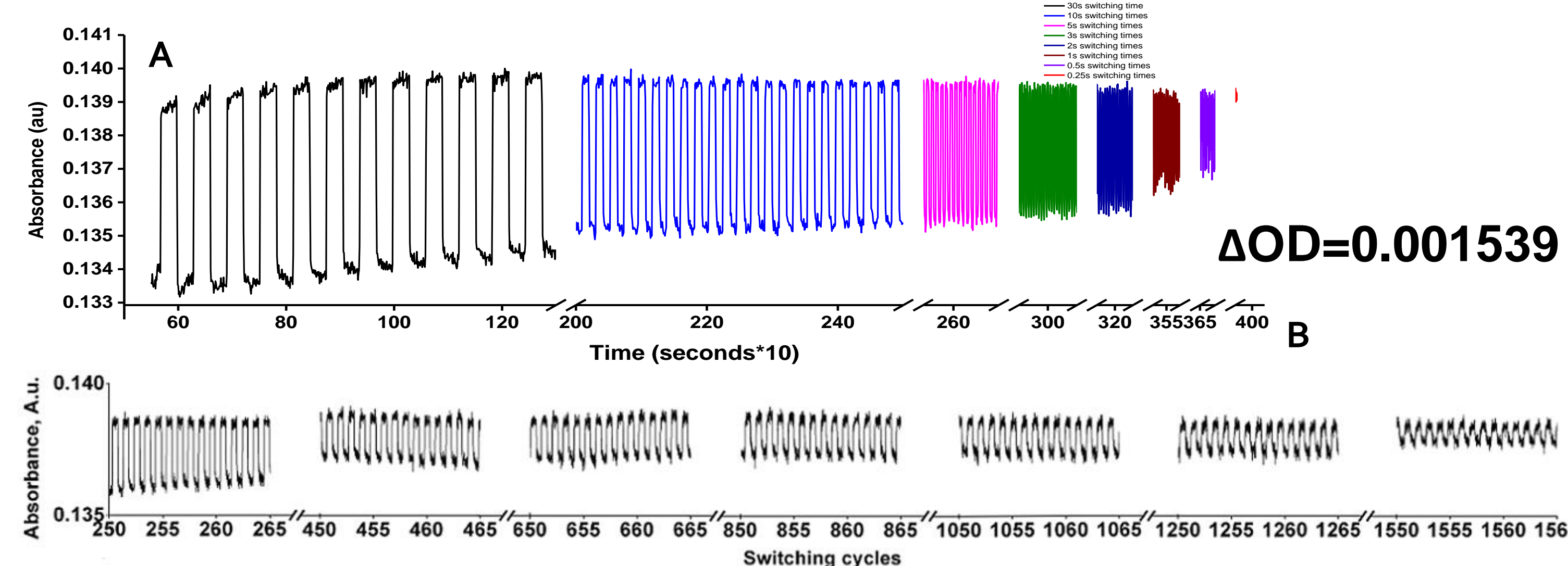


Figure 6: the spectroelectrochromic data for the bisterpyridine assembly. A) the switching time cycles. B) subsections of the long term cycling for 48 hours.

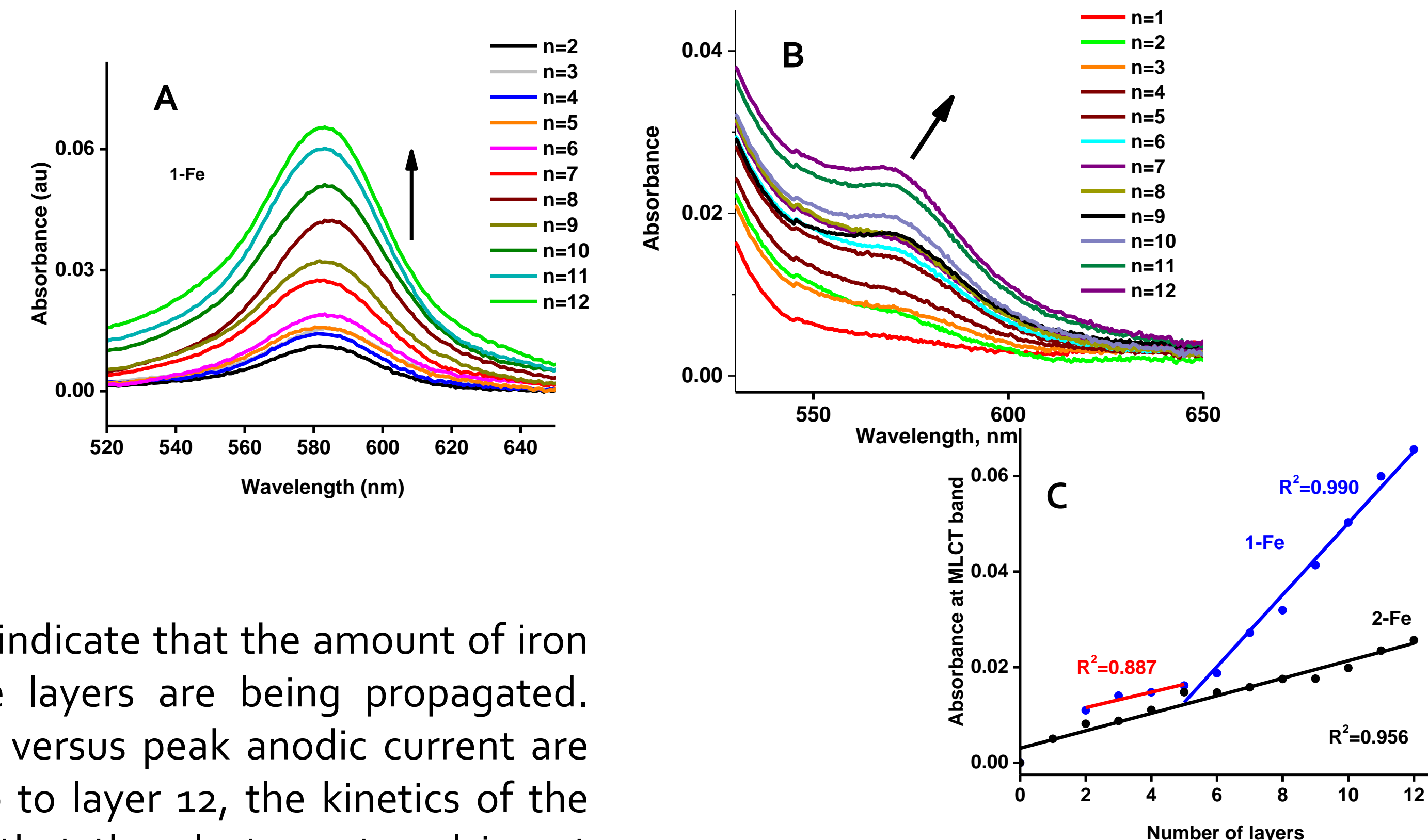


Figure 7: the UV-Visible results for all layers. A) the bisterpyridine assembly. B) the triazine terpyridine assembly. C) a comparison of the peak growth for both assemblies.

References

1-Yang, P., Sun, P., & Mai, W. (2016). Electrochromic energy storage devices. *Materialstoday*, 19(7), 394-402. doi:https://doi.org/10.1016/j.mattod.2015.11.007

Acknowledgements

NSERC, UOIT, both the Zenkina and Easton groups

